JOURNAL OF VIROLOGY, Aug. 1994, p. 5204–5215
0022-538X/94/$04.00+0

Vol. 68, No. 8

Intracellular Manipulation of Disulfide Bond Formation in Rotavirus Proteins during Assembly

LENNART SVENSSON,[1,2]* PHILIP R. DORMITZER,[1,2] CARL-HENRIK VON BONSDORFF,[3] LEENA MAUNULA,[3] AND HARRY B. GREENBERG[1,2]

Division of Gastroenterology and Department of Microbiology and Immunology, Stanford University Medical Center, Stanford, California 94305[1]; Palo Alto Veterans Administration Medical Center, Palo Alto, California 94304[2]; and Haartman Institute, Department of Virology, University of Helsinki, Helsinki, Finland[3]

Received 7 February 1994/Accepted 13 May 1994

Rotavirus undergoes a unique mode of assembly in the rough endoplasmic reticulum (RER) of infected cells. Luminal RER proteins undergo significant cotranslational and posttranslational modifications, including disulfide bond formation. Addition of a reducing agent (dithiothreitol [DTT]) to rotavirus-infected cells did not significantly inhibit translation or disrupt established disulfide bonds in rotavirus proteins but prevented the formation of new disulfide bonds and infectious viral progeny. In DTT-treated, rotavirus-infected cells, all vp4, vp6, and ns28 epitopes but no vp7 epitopes were detected by immunohistochemical staining with a panel of monoclonal antibodies. When oxidizing conditions were reestablished in DTT-treated cells, intramolecular disulfide bonds in vp7 were rapidly and correctly established with the restoration of antigenicity, although prolonged DTT treatment led to the accumulation of permanently misfolded vp7. Electron microscopy revealed that cytosolic assembly of single-shelled particles and budding into the ER was not affected by DTT treatment but that outer capsid assembly was blocked, leading to the accumulation of single-shelled and enveloped intermediate subviral particles in the RER lumen.

Rotavirus, a member of the *Reoviridae*, undergoes a unique maturation process in the endoplasmic reticulum (ER). The assembly process, which includes translocation of subviral particles across the ER membrane and retention of mature virus in the ER, has provided a system in which posttranslational events, such as protein targeting and retention, can be studied.

During viral maturation, single-shelled particles, assembled from vp1, vp2, vp3, and vp6 in the cytoplasm, interact with ns28, a virus-encoded transmembrane protein that resides in the ER and that functions as a receptor for vp6 (5, 37). As the single-shelled particle buds through the ER membrane, it transiently acquires an ER membrane-derived envelope. It appears that in the ER, the enveloped particle loses this membrane and acquires an outer capsid, consisting of vp7 and vp4 (1, 3). The mechanisms of translocation across the ER, loss of the lipid envelope, and acquisition of properly folded outer capsid proteins remain largely unresolved. In fact, the possibility of an alternate assembly pathway that bypasses the enveloped intermediate stage has recently been raised (48).

The rough ER (RER), where these events take place, is the site for synthesis of resident and secretory proteins. In the RER, proteins may acquire several posttranslational modifications, such as N- and O-linked glycosylation, which are essential for the proper folding and maturation of some proteins (17, 20). The ER is also a major intracellular calcium reservoir. Calcium plays a prominent role in rotavirus maturation. Specifically, depletion of calcium from the ER blocks rotavirus budding at the transient enveloped stage (44) and prevents the formation of heterooligomers between vp7, vp4, and ns28 (35, 43). Calcium is required for the proper folding of vp7 (15), and baculovirus-expressed rotavirus ns28 alters intracellular calcium levels (52).

It is well-known that proteins can fold spontaneously in vitro (4), but it has recently been established that protein folding in vivo is assisted (30) by at least two classes of proteins. Molecular chaperones (22) recognize and stabilize partially folded intermediates during polypeptide folding. Protein disulfide isomerase, an ER-associated protein, promotes disulfide bond formation and facilitates the rapid reshuffling of incorrect disulfide pairings (21). Disulfide bonds between cysteines are crucial for the maintenance of folding and stability of many proteins (14, 50). In the case of influenza virus hemagglutinin, disulfide bond formation and folding begin on the nascent polypeptide chain (9). Other viral proteins, such parainfluenza virus hemagglutinin, fold and oligomerize before acquiring the correct intramolecular disulfide bonds (11).

While the importance of calcium in rotavirus assembly and antigenicity (15, 38, 43, 45) has been addressed, the importance of disulfide bonds for rotavirus protein folding and assembly has not been examined as thoroughly. Several researchers have reported that the trimeric inner capsid protein of rotavirus, vp6, contains disulfide bonds (8, 19, 24, 40, 44). Two disulfide linkages have been mapped in the rotavirus spike protein, vp4 (40). The vp7 protein associated with and retained in the ER has intramolecular disulfide bonds (24, 40). It has also been suggested that disulfide bonds are responsible for the oligomerization of ns28 (35).

While protein folding may be studied in vitro, such experiments may not accurately reflect the process of protein folding in the cell. Protein folding and disulfide bond formation can be studied in vivo by adding a reducing agent such as dithiothreitol (DTT) or β-mercaptoethanol to living cells (2, 10). It has recently been reported that disulfide bond formation in the asialoglycoprotein receptor, influenza virus hemagglutinin, vesicular stomatitis virus G protein, and mouse hepatitis virus S protein can be manipulated in this manner without blocking

* Corresponding author. Present address: Department of Virology, Swedish Institute for Infectious Disease Control, Karolinska Institute, 105 21 Stockholm, Sweden. Phone: 46-8 7351228. Fax: 46-8 7303248.

critical cellular functions (10, 13, 34, 39, 51). In the present study, we have examined the importance of disulfide bond formation during rotavirus replication by adding DTT to rotavirus-infected cells.

MATERIALS AND METHODS

Cells, viruses, and antibodies. MA104 cells were grown in medium 199 or Dulbecco's modified Eagle's minimal essential medium supplemented with 10% fetal calf serum. Rhesus rotavirus (RRV) was obtained from infected cells by freeze-thawing. The monoclonal antibodies (MAbs) used in this study are presented in Table 2 and include the following: 159, 4F8, and 96 recognize vp7 and neutralize RRV (26, 47); M60 recognizes a cross-reacting, nonneutralizing epitope on vp7 (47); M2, M7, M11, 5D9, 5C4, 1A9, 7A12, and 2G4 recognize vp4 and neutralize RRV (36, 47); 255/60 recognizes trimeric vp6 (25, 32), and B4/55 recognizes ns28 (42). GP962 and R1 are hyperimmune guinea pig and rabbit sera against RRV, respectively. MB7 is a polyclonal mouse serum that efficiently immunoprecipitates RRV vp7.

Rotavirus infection, plaquing, HA, and antigen detection. RRV was activated with 5 μg of trypsin per ml for 30 min at 37°C before inoculation of cultures. MA104 cells were infected in serum-free medium. After a 1-h incubation, inoculae were removed and replaced with fresh medium. The titers of RRV were determined by a plaque assay on serum-free cell culture medium with 0.6% agarose and 0.5 μg of trypsin per ml added. Hemagglutination (HA) assays with human type O erythrocytes were performed as previously described (32). Rotavirus antigen was detected by a previously described enzyme-linked immunosorbent assay (ELISA) (16). Briefly, a rotavirus-infected cell lysate was diluted 1:5 with phosphate-buffered saline (PBS) and incubated overnight at 4°C in an ELISA plate. Unsaturated binding sites were blocked with PBS and 10% fetal calf serum overnight at 4°C. Bound antigen was detected by GP962 and peroxidase-linked goat antibody against guinea pig immunoglobulin G (Kirkegaard and Perry Laboratories, Gaithersburg, Md.).

Immunoperoxidase staining. Prior to fixation, rotavirus-infected MA104 cell monolayers were incubated with ice-cold PBS containing 40 mM *N*-ethylmaleimide (NEM) for 2 min to prevent the rearrangement of disulfide bonds (12). Then, the cells were fixed with 3% paraformaldehyde in PBS for 2 h at room temperature, and the cell membranes were made permeable by treatment with 0.5% Triton X-100 in PBS for 10 min. PBS containing 0.2% bovine serum albumin (BSA) and 0.1% Triton X-100 was used to dilute the antibodies and to wash the cells. Fixed monolayers were incubated with primary antibody for 2 h at 37°C, washed twice, and then incubated with peroxidase-labeled goat antibody against mouse immunoglobulin G (Kirkegaard and Perry Laboratories) for 1 h at 37°C. After two more washes, the cell layers were stained with aminoethylcarbazole as previously described (28).

Metabolic labeling of infected-cell proteins. To produce metabolically labeled lysates, MA104 cells were inoculated with trypsin-activated RRV at a multiplicity of infection (MOI) of 5. Infected cells were starved for 1 h in methionine-free medium before pulse-labeling with 50 μCi of [^{35}S]methionine per ml for various periods. For chase experiments, the cell layers were then washed and incubated with medium containing 10 mM methionine and 0.7 mM cycloheximide. At the end of a radioactive pulse or after a chase, cells were incubated with ice-cold PBS with 40 mM NEM for 2 min. Cells were then lysed in ice-cold lysis buffer (10 mM Tris-HCl [pH 7.5], 150 mM NaCl, 1% Triton X-100, 0.5% sodium dodecyl sulfate [SDS], 6 μg of leupeptin per ml, 3 μg of antipain per ml, 10 μg of chymostatin per ml). Lysates were cleared of cell debris by centrifugation at 13,000 × *g* for 5 min in a microcentrifuge. To obtain labeled proteins synthesized in the presence of DTT, various amounts of DTT were added 5 min before the [^{35}S]methionine pulse and were maintained through the chase. In reoxidation experiments, pulse-labeling in DTT-containing medium was followed by two washes with and incubation in DTT-free chase medium for various periods. To inhibit glycosylation, 2 μg of tunicamycin (Boehringer Mannheim, Indianapolis, Ind.) per ml was added to the starvation, pulse, and chase media.

Rotavirus purification. For virus purification, MA104 cells were infected with RRV at an MOI of 5. From 4 to 10 h postinfection (p.i.), the cells were incubated in methionine-free medium supplemented with 100 μCi of [^{35}S]methionine per ml. The cells were harvested in serum-free medium at 20.5 h after infection, frozen and thawed three times, and sonicated briefly. The supernatant of a low-speed spin of the lysate (13,000 × *g* for 5 min in a microcentrifuge) and a trichlorotrifluoroethane extract of the pellet resulting from low-speed centrifugation were pooled and pelleted at high speed (287,500 × *g*) for 1 h in an SW55 rotor (Beckman Instruments, Palo Alto, Calif.). This pellet was washed and resuspended in TNC (10 mM Tris-Cl [pH 7.5], 100 mM NaCl, 1.5 mM $CaCl_2$), and the resulting solution was layered over a 1.37-g/ml CsCl solution in TNC and centrifuged for 22.5 h at 85,500 × *g* at 20°C in an SW55 rotor. Fractions were collected by bottom puncture, and fractions containing double-shelled rotavirus particles were identified by scintillation counting and measurement of refractive index.

Immunoprecipitation. Immunoprecipitation from radiolabeled infected-cell lysates was performed essentially as previously described (49). Briefly, 50-μl portions of radiolabeled lysates were incubated with 1 μl of antibody and 450 μl of RIPA buffer (10 mM Tris-Cl [pH 7.5], 0.15 M NaCl, 0.6 M KCl, 4 mM EDTA, 1% Triton X-100) overnight at 4°C. Then, 25 μl of *Staphylococcus aureus* protein A–Sepharose CL-4B (Pharmacia, Uppsala, Sweden) was added to the mixture and incubated for 1 h at room temperature on a rocker platform. The protein A-Sepharose-coupled immune complexes were pelleted at 13,000 × *g* for 30 s in a microcentrifuge and washed four times in RIPA buffer and twice in 10 mM Tris-HCl (pH 8.0)–150 mM NaCl. The immune complexes were suspended in 30 μl of nonreducing sample buffer (10 mM Tris-HCl [pH 6.8], 0.5% SDS, 10% glycerol) or reducing sample buffer (nonreducing sample buffer with 1% β-mercaptoethanol added). Unless otherwise indicated, samples were boiled for 3 min before separation by SDS-polyacrylamide gel electrophoresis (PAGE).

SDS-PAGE. Polypeptide separation was performed by SDS-PAGE using a 4.5% stacking gel and a 10% separation gel, essentially as previously described (49). Electrophoresis was carried out at a constant voltage of 65 V at room temperature, followed by fixation with 10% (vol/vol) glacial acetic acid and 30% (vol/vol) methanol. Autoradiography was performed as previously described (49). The apparent molecular weights were determined by comparison of the relative mobilities of the rotavirus polypeptides and molecular mass standards. The standards used were ^{14}C-methylated proteins (Amersham Corp., Arlington Heights, Ill.): myosin 200,000 (200 kDa), phosphorylase *b* (97.4 kDa), BSA (69 kDa), ovalbumin (46 kDa), carbonic anhydrase (30 kDa), and lysozyme (14.3 kDa).

Electron microscopy. Monolayers of MA104 cells in 5-cm-diameter petri dishes were infected with RRV at an MOI of 5 and treated with DTT as described above. The monolayers

TABLE 1. Effect of DTT treatment of rotavirus particles on HA and infectivity[a]

DTT concn (mM)	HA titer[b]	Infectivity	
		Titer	Post-R1 titer[c]
0	2,564	3.5×10^7	2.0×10^4
1	1,282	2.1×10^7	4.1×10^4
5	1,282	ND[d]	ND
10	1,282	2.3×10^7	5.6×10^4

[a] RRV samples were incubated with the indicated concentrations of DTT for 30 min at 37°C before the assay. The entire HA assay and absorption and cell entry in the assay were performed in the presence of the indicated concentration of DTT.

[b] HA titers are expressed as the reciprocal of the highest dilution showing complete HA.

[c] Titer after 15-min incubation of virus with 1:1,000 dilution of R1 (rabbit hyperimmune serum against RRV) in the presence of the indicated concentration of DTT.

[d] ND, not done.

were then fixed with 2.5% glutaraldehyde in 0.1 M cacodylate buffer, pH 7.4. The cells were scraped off in the fixative and pelleted at 10,000 × *g* for 2 min. Postfixation was performed in 1% osmium tetroxide for 1 h, followed by staining with uranyl acetate. After dehydration, the samples were embedded in Epon 812. Thin sections were examined with a Jeol CX-100 II electron microscope.

RESULTS

Effects of DTT treatment of rotavirus particles on HA and infectivity. To determine if the conditions that we used to study vp7 synthesis affected rotavirus virions, RRV stocks were treated with 1 to 10 mM DTT for 30 min at 37°C. Following DTT treatment, the stocks were used in HA assays with the indicated amounts of DTT present throughout the assay (Table 1). Treatment with increasing amounts of DTT had no significant effect on the HA titers of the stocks. The titers of the DTT-treated stocks were also determined by a plaque assay on MA104 cells. The different concentrations of DTT were maintained in the medium for 30 min after inoculation to maintain reducing conditions during viral absorption and penetration, following which extracellular virus was inactivated by incubating the monolayers for 15 min at 37°C in the presence of DTT with a 1:1,000 dilution of R1, a polyclonal rabbit antiserum against RRV. The DTT-treated stocks showed no significant decrease in titer relative to those of the non-treated stocks (Table 1). No difference was noted in the ability of a 1:1,000 dilution of R1 to neutralize extracellular virus in the presence or absence of DTT (Table 1).

Effects of DTT treatment of virus particles on disulfide bonds. Since the above DTT treatments did not affect RRV HA or infectivity, we asked whether DTT at the concentrations employed reduced the disulfide bonds in the particles. [^{35}S]methionine-labeled, CsCl-purified, double-shelled, trypsinized particles separated by nonreducing SDS-PAGE yielded the expected pattern of viral structural proteins, except that the vp6 band was heterogeneous (Fig. 1, lane 1). Treatment of the particles with 20 mM NEM before nonreducing SDS-PAGE analysis (Fig. 1, lane 2) resulted in tightening of the vp6 band, indicating that in the absence of NEM, rearrangement of vp6 disulfide bonds occurs during sample preparation. Incubation of the purified particles with 1 or 10 mM DTT for 30 min at

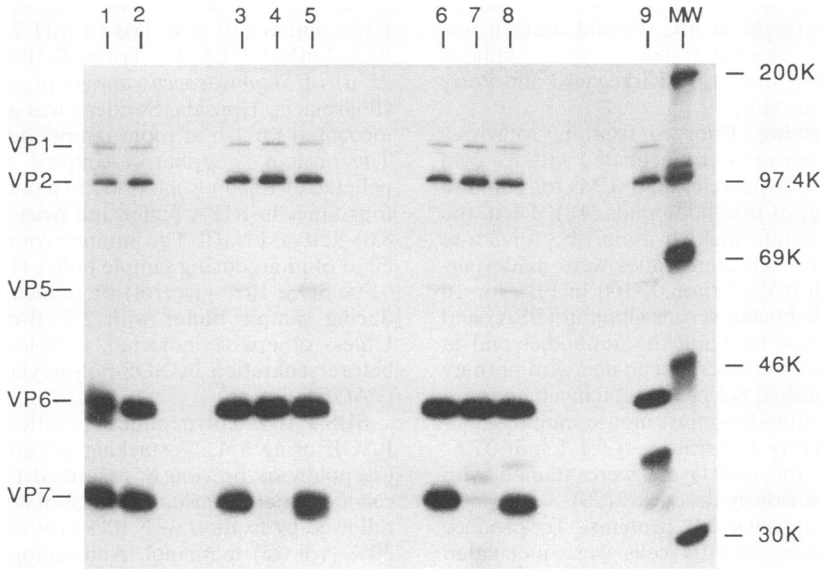

FIG. 1. Effects of DTT on intact and disrupted purified rotavirus particles. [^{35}S]methionine-labeled, CsCl-purified RRV particles were dialyzed against TNC and trypsinized. Before the samples were boiled for 2 min and separated by SDS-PAGE, they were incubated under the following conditions: 20 mM EDTA at room temperature (RT) for 5 min, nonreducing sample buffer (62.5 mM Tris-Cl [pH 6.8], 2% SDS, 20% glycerol, 0.002% bromphenol blue) at RT for 5 min, reducing sample buffer (with 0.5% β-mercaptoethanol) at RT for 5 min, 1 or 10 mM DTT at 37°C for 30 min, and 20 mM NEM at 37°C for 3 min. The conditions applied to individual samples, listed in order of application, are as follows: nonreducing sample buffer (lane 1); NEM and nonreducing sample buffer (lane 2); 1 mM DTT, NEM, and nonreducing sample buffer (lane 3); EDTA, 1 mM DTT, NEM, and nonreducing sample buffer (lane 4); nonreducing sample buffer, EDTA, 1 mM DTT, and NEM (lane 5); 10 mM DTT, NEM, and nonreducing sample buffer (lane 6); EDTA, 10 mM DTT, NEM, and nonreducing sample buffer (lane 7); nonreducing sample buffer, EDTA, 10 mM DTT, and NEM (lane 8); and reducing sample buffer (lane 9). Molecular weight markers (in thousands [K]) in reducing sample buffer are shown in lane MW.

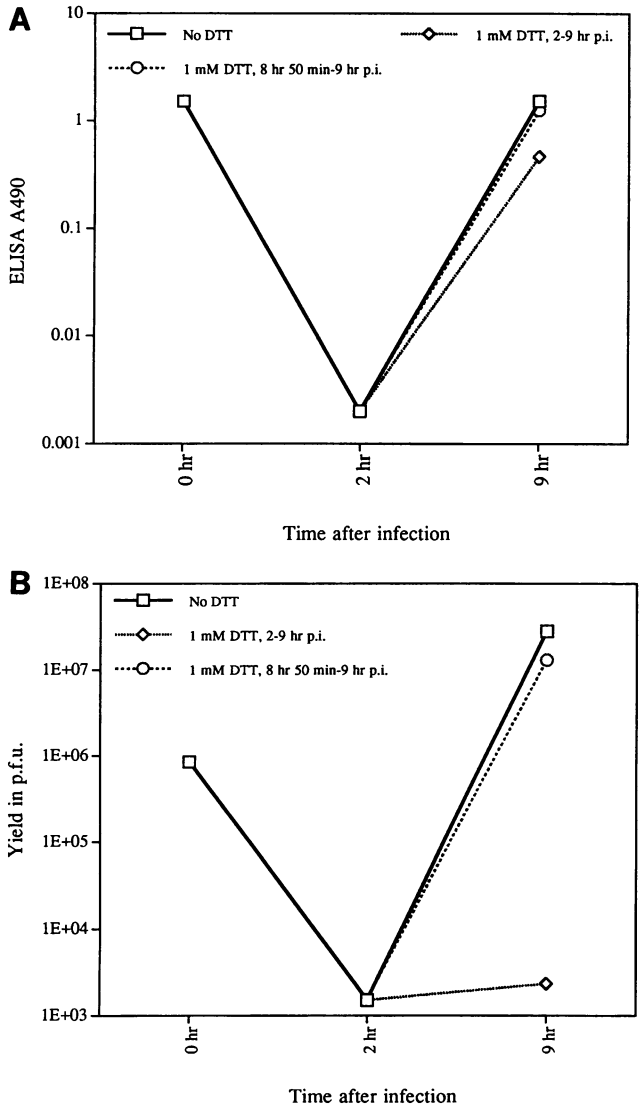

FIG. 2. Effects of in vivo DTT treatment on rotavirus antigen and infectious yield from RRV-infected MA104 cells. MA104 cells were infected with RRV at an MOI of 5. An aliquot of the inoculum was treated with 20 mM NEM for 3 min at room temperature, then diluted to 250 μl in cell culture medium, and set aside for antigen and infectivity assays (0-h sample). At 1 h p.i., the infected monolayers were washed and incubated with a 1:500 dilution of R1, a hyperimmune rabbit serum against RRV, at 37°C for 1 h. At 2 h p.i., all monolayers were washed three times with medium. One infected monolayer was then treated with 20 mM NEM in cell culture medium and harvested in 250 μl of medium (2-h sample). The remaining infected monolayers were treated with 1 mM DTT from 2 to 9 h p.i. or with 1 mM DTT from 8 h 50 min p.i. to 9 h p.i. or were left untreated. These monolayers were treated with NEM and harvested at 9 h p.i. as described above (9-h samples). All samples were freeze-thawed three times and trypsinized before further analysis. (A) Antigen yield determined by direct coat ELISA reported as A_{490} units above the average, value obtained by using ELISA buffer alone and an uninfected MA104 cell lysate for antigen. (B) Infectious virus yield, determined by plaque assay.

TABLE 2. Immunoperoxidase staining of RRV-infected, DTT-treated MA104 cells[a]

MAb	Protein detected[b]	Staining[c] after DTT treatment		
		10-min, 1–5 mM, 12 h p.i.	10 min, 1–25 mM, 7 h p.i.	0.5 mM, 2–7 h p.i.
B4/55	ns28	+	+	(+)
255/60	vp6	+	+	+
2G4	vp4 (vp5)	+	+	+
M2	vp4 (vp5)	+	+	+
M7	vp4 (vp5)	+	+	+
5D9	vp4 (vp8)	+	+	+
5C4	vp4 (vp8)	+	+	+
1A9	vp4 (vp8)	+	+	(+)
M11	vp4 (vp8)	+	+	+
7A12	vp4 (vp8)	+	+	+
M60	vp7	+	+	−
4C3	vp7	+	+	−
159	vp7	+	+	−
4F8	vp7	+	+	−

[a] Cells were treated with NEM, fixed, and immunoperoxidase stained immediately after DTT treatment, as described in Materials and Methods.
[b] vp5 and vp8 are trypsin cleavage products of vp4.
[c] Symbols: +, more than 30% of staining observed in non-DTT-treated controls. (+), 2 to 30% of staining in controls, −, less than 2% of staining in controls.

37°C before the addition of 20 mM NEM caused no shift in the mobility of rotavirus structural proteins (Fig. 1, lanes 3 and 6).

To determine whether only proteins in intact particles showed this resistance to DTT treatment, the particles were disrupted by incubation in SDS-containing nonreducing sample buffer with 20 mM EDTA added before DTT and NEM treatment. With these dissociated rotavirus structural proteins, 1 mM DTT treatment (Fig. 1, lane 5) caused only a slight dispersion of the vp7 band; 10 mM DTT treatment (Fig. 1, lane 8) caused a shift to a slightly greater mobility in the major vp7 band and the appearance of a minor band with retarded mobility on an SDS-polyacrylamide gel. This minor vp7 band comigrated with the major fully reduced vp7 band obtained by boiling the sample in the presence of 0.5% β-mercaptoethanol and in the absence of NEM (Fig. 1, lane 9). When particles were treated with EDTA in the absence of SDS-containing sample buffer, the solubilized outer capsid proteins were degraded by trypsin (Fig. 1, lanes 4 and 7). It appears that established disulfide bonds in rotavirus particles were resistant to DTT at the concentrations used. There was a modest increase in the sensitivity of vp7 disulfide bonds to DTT treatment upon particle disruption, possibly because conformational changes in vp7 induced by detergent (in the sample buffer) or calcium chelation make its disulfide bonds more accessible to reduction. The decreased mobility of fully reduced vp7 suggests that intramolecular disulfide bonds in vp7 cause it to assume a more compact structure.

DTT treatment of rotavirus-infected cells blocks production of infectious rotavirus. Preliminary experiments confirmed that as has been observed in other cell types (10, 51), DTT treatment did not prevent protein translation in MA104 cells or reduce cell viability (data not shown). Given that 1 mM DTT treatment did not significantly inhibit protein synthesis in MA104 cells or disrupt established disulfide bonds in rotavirus particles, we examined the effects of 1 mM DTT treatment from 2 to 9 h p.i. on the production of rotavirus antigen and rotavirus infectious particles from RRV-infected MA104 cells (MOI of 5). Aliquots of the same samples were used for the determination of antigen and infectious particle yields. In vivo

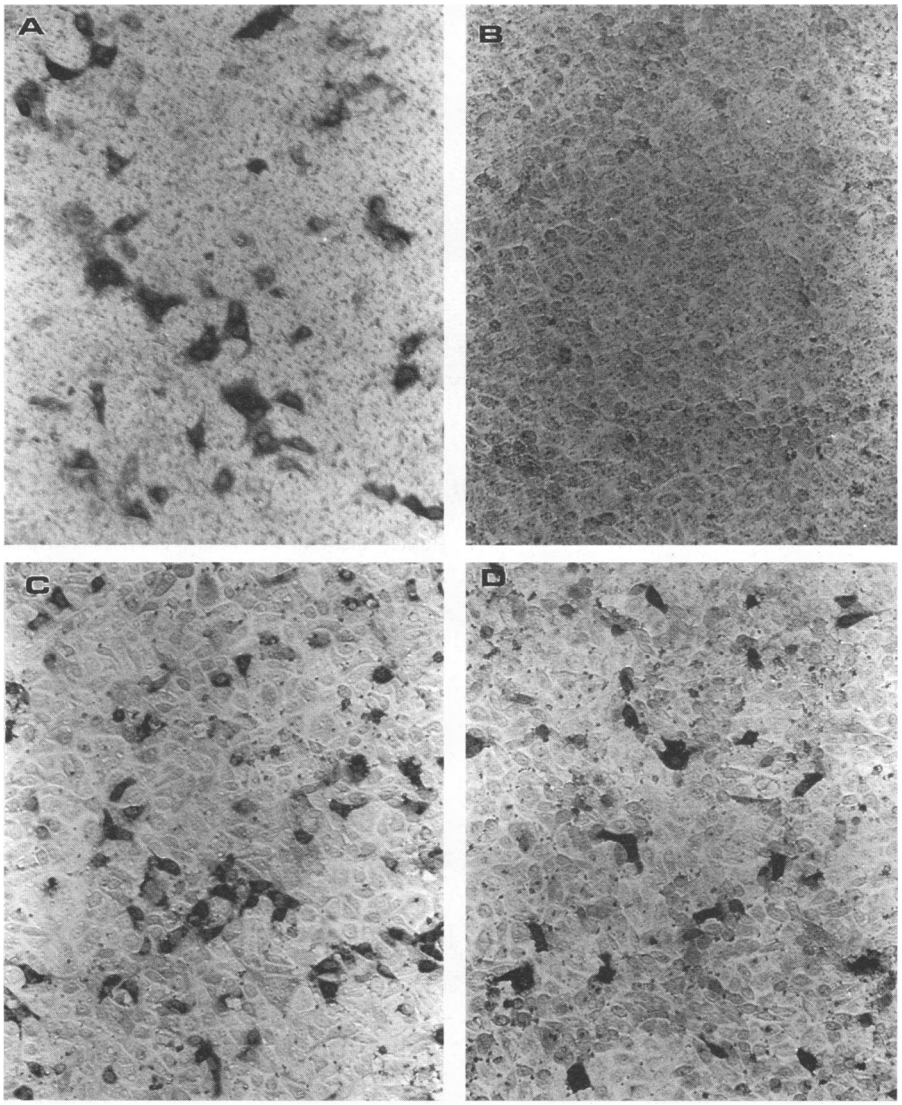

FIG. 3. Immunoperoxidase staining of DTT-treated and non-DTT-treated RRV-infected MA104 cells. MA104 cells were infected with RRV at an MOI of 0.1. For DTT treatment, cells were incubated in medium containing 0.5 mM DTT from 2 to 7 h p.i. All monolayers were washed with ice-cold PBS containing 40 mM NEM before paraformaldehyde fixation at 7 h p.i. and immunoperoxidase staining. (a) No DTT, stained with MAb M60 (vp7 specific). (b) Treated DTT with and stained with MAb M60. (c) No DTT, stained with MAb 255/60 (vp6 specific). (d) Treated with DTT and stained with MAb 255/60.

DTT treatment during infection caused only a moderate drop in the yield of rotavirus antigen detected by ELISA (Fig. 2A); however, this treatment caused a 4.1-log-unit drop in the yield of infectious rotavirus particles detected in a plaque assay (Fig. 2B). A 10-min pulse of 1 mM DTT just before harvesting had little effect on the yield of viral antigen (Fig. 2A) or infectious viral particles (Fig. 2B). Therefore, it appears that DTT treatment of infected cells blocked viral assembly without disrupting already assembled particles and without severely affecting total viral protein synthesis.

Treatment of rotavirus-infected cells with DTT alters the antigenicity of the ER-associated vp7. To define the block to rotavirus assembly in greater detail, the effect of DTT on the antigenicity of RRV proteins was examined. Specifically, RRV-infected MA104 cells were treated with DTT, briefly incubated with 20 to 40 mM NEM, fixed with paraformaldehyde, and immunoperoxidase stained with several MAbs against rotavirus proteins. A 10-min pulse with 1 mM DTT followed directly by NEM treatment and fixation at 7 or 12 h p.i. did not significantly reduce staining for the epitopes recognized by vp4-, vp6-, vp7- or ns28-specific MAbs (Table 2). Incubation with 0.5 mM DTT from 2 h p.i. until fixation at 7 h p.i. caused only a modest decrease in staining for epitopes present on vp4 and vp6 (Table 2 and Fig. 3). This modest drop in staining is consistent with the moderate decrease in ELISA-detectable rotavirus antigen observed after prolonged DTT treatment (Fig. 2A). In contrast, addition of 0.5 mM DTT to infected cells from 2 h p.i. until NEM treatment and fixation at 7 h p.i. eliminated all staining with neutralizing and nonneutralizing MAbs against vp7 (Table 2 and Fig. 3). The vp4-specific epitope recognized by MAb 1A9 and the ns28 epitope recognized by MAb B4 showed intermediate levels of loss upon DTT treatment (Table 2). The loss of not only the calcium-dependent vp7 epitopes recognized by neutralizing

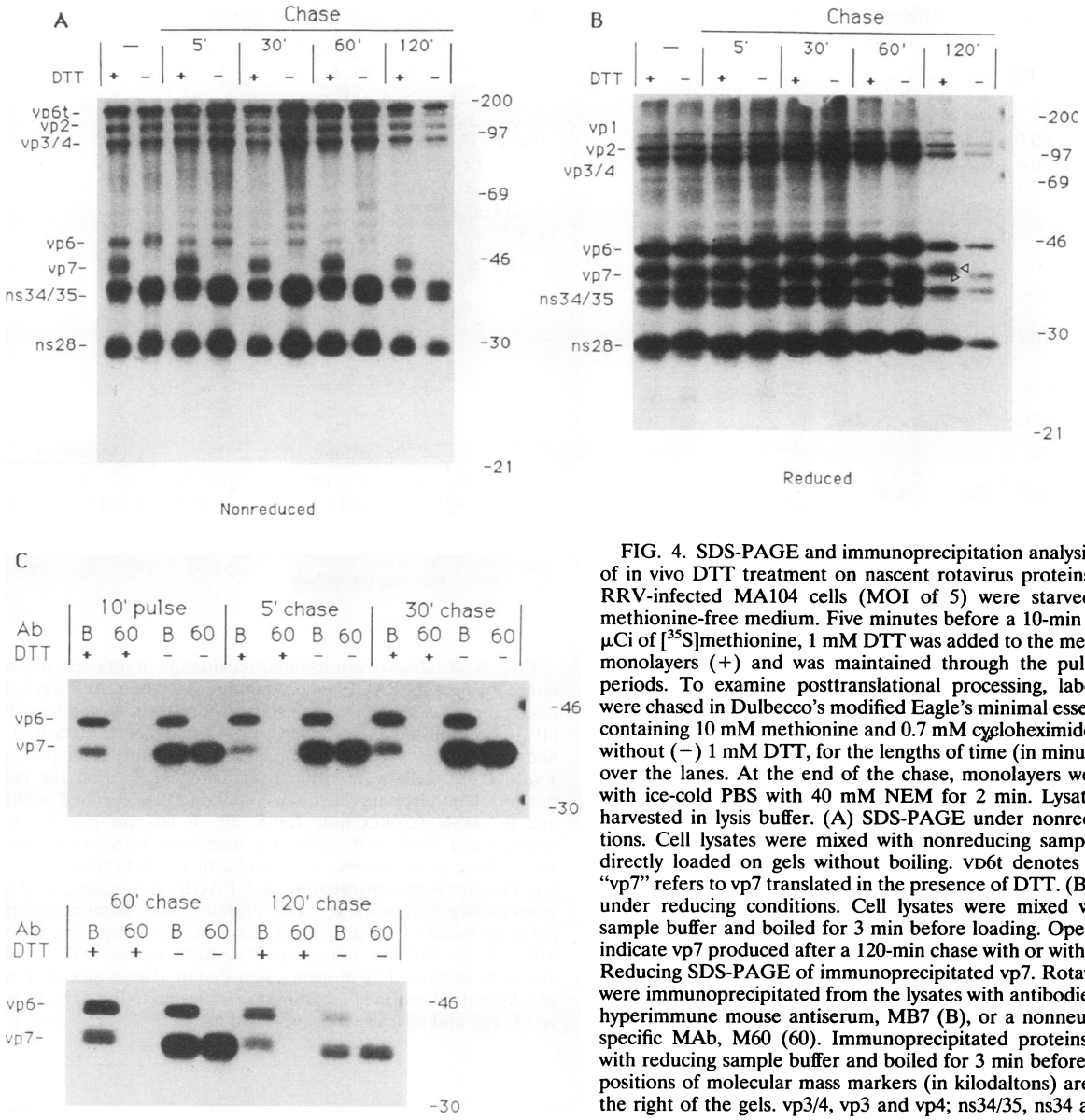

FIG. 4. SDS-PAGE and immunoprecipitation analysis of the effect of in vivo DTT treatment on nascent rotavirus proteins. At 7 h p.i., RRV-infected MA104 cells (MOI of 5) were starved for 1 h in methionine-free medium. Five minutes before a 10-min pulse with 50 μCi of [^{35}S]methionine, 1 mM DTT was added to the medium of some monolayers (+) and was maintained through the pulse and chase periods. To examine posttranslational processing, labeled proteins were chased in Dulbecco's modified Eagle's minimal essential medium containing 10 mM methionine and 0.7 mM cycloheximide, with (+) or without (−) 1 mM DTT, for the lengths of time (in minutes) indicated over the lanes. At the end of the chase, monolayers were incubated with ice-cold PBS with 40 mM NEM for 2 min. Lysates were then harvested in lysis buffer. (A) SDS-PAGE under nonreducing conditions. Cell lysates were mixed with nonreducing sample buffer and directly loaded on gels without boiling. VD6t denotes trimeric vp6. "vp7" refers to vp7 translated in the presence of DTT. (B) SDS-PAGE under reducing conditions. Cell lysates were mixed with reducing sample buffer and boiled for 3 min before loading. Open arrowheads indicate vp7 produced after a 120-min chase with or without DTT. (C) Reducing SDS-PAGE of immunoprecipitated vp7. Rotavirus proteins were immunoprecipitated from the lysates with antibodies (Ab), i.e., a hyperimmune mouse antiserum, MB7 (B), or a nonneutralizing vp7-specific MAb, M60 (60). Immunoprecipitated proteins were mixed with reducing sample buffer and boiled for 3 min before loading. The positions of molecular mass markers (in kilodaltons) are indicated to the right of the gels. vp3/4, vp3 and vp4; ns34/35, ns34 and ns35.

MAbs 159, 4C3, and 4F8 but also the calcium-independent vp7 epitope recognized by nonneutralizing MAb M60 was surprising, since the latter epitope is resistant to SDS treatment and methanol fixation (16). The absence of an effect of DTT treatment late in infection on vp7 antigenicity confirms that established disulfide bonds in rotavirus structural proteins are resistant to reduction by modest concentrations of DTT.

SDS-PAGE analysis of rotavirus protein synthesis in the presence of DTT. To further explore the effects of DTT treatment of rotavirus-infected cells on individual rotavirus proteins, radiolabeled RRV-infected MA104 cell lysates were produced by adding 1 mM DTT to infected cells 5 min before a radioactive pulse and maintaining DTT through the pulse and chase periods. Radiolabeled rotavirus proteins from these lysates and from lysates of non-DTT-treated controls were analyzed by nonreducing SDS-PAGE, reducing SDS-PAGE, and reducing SDS-PAGE and immunoprecipitation (Fig. 4A, B, and C, respectively). When proteins in nonboiled lysates from DTT-treated cells were analyzed by nonreducing SDS-PAGE, vp6 remained multimeric (Fig. 4A), suggesting that disulfide bonds were not required for trimer formation or that disulfide bonds were maintained despite DTT treatment during vp6 synthesis and oligomerization. Preventing the formation of disulfide bonds on nascent vp7, on the other hand, had a pronounced effect on its conformation (Fig. 4A). In lysates produced in non-DTT-treated cells, vp7 with disulfide bonds comigrated with ns34 and ns35 (Fig. 4A). DTT treatment of the cells prevented the formation of disulfide bonds on vp7, resulting in a decrease in its electrophoretic mobility, like that seen upon boiling vp7 in 0.5% β-mercaptoethanol (Fig. 1, lane 9).

When the rotavirus-infected, radiolabeled cell lysates were reduced by boiling in 0.5% β-mercaptoethanol before SDS-PAGE analysis (Fig. 4B), there remained small differences in the electrophoretic mobilities of DTT-treated and non-DTT-treated vp7. Specifically, while the electrophoretic mobility of

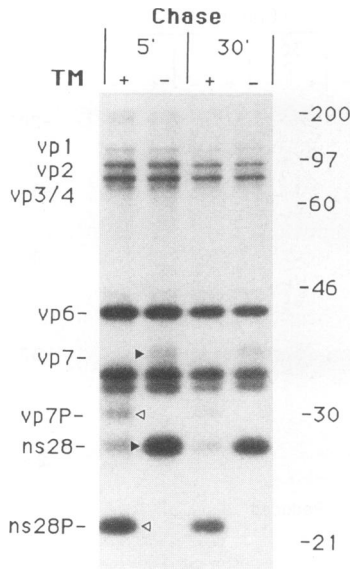

FIG. 5. Effect of in vivo reduction on the glycosylation of rotavirus proteins. At 7 h p.i., rotavirus-infected cells were starved for 1 h in methionine-free medium with (+) or without (−) 2 μg of tunicamycin (TM) per ml. Five minutes before a 10-min pulse with 50 μCi of [^{35}S]methionine, 1 mM DTT was added to the medium. Labeled proteins were chased with Dulbecco's modified Eagle's minimal essential medium supplemented with 10 mM methionine, 0.7 mM cycloheximide, and 1 mM DTT. After the 5-min (5′) or 30-min (30′) chase, cells were briefly incubated with 20 mM NEM in PBS, lysed, and separated by SDS-PAGE under reducing conditions. The positions of molecular mass markers (in kilodaltons) are indicated to the right of the gel. Filled arrowheads indicate glycosylated forms and empty arrowheads indicate precursor forms of vp7 (vp7P) and ns28 (ns28P). vp3/4, vp3 and vp4.

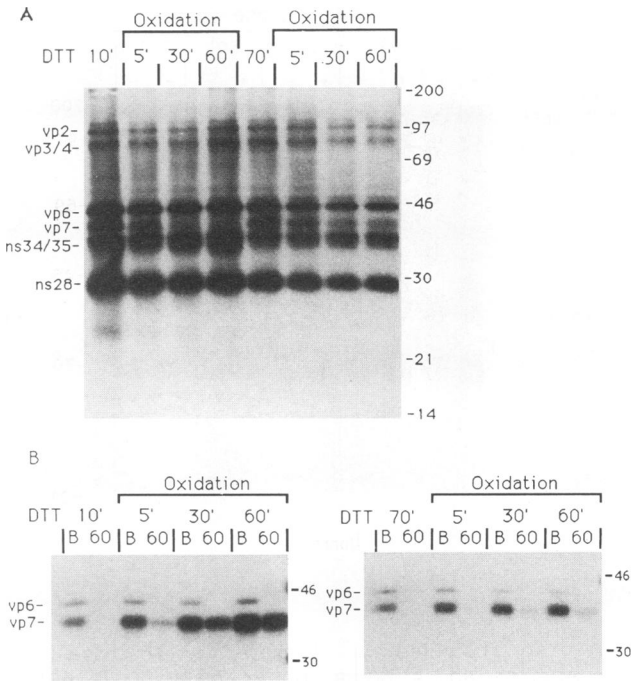

FIG. 6. Analysis of intracellular reoxidation of rotavirus proteins by nonreducing SDS-PAGE and immunoprecipitation. At 7 h p.i., RRV-infected cells were methionine starved for 1 h, followed by a 10-min (10′) or 70-min (70′) (indicated to the left of the oxidation brackets above the lanes) [^{35}S]methionine pulse (50 μCi/ml) in the presence of 1 mM DTT. Cells were either lysed immediately after the pulse or reoxidized in cell culture medium containing 10 mM added methionine and 0.7 mM cycloheximide for 5, 30, or 60 min (5′, 30′, or 60′, respectively) (indicated under the oxidation brackets) before lysis. Before lysis, monolayers were washed with ice-cold PBS–40 mM NEM. (A) Proteins were separated by SDS-PAGE after boiling for 3 min in nonreducing sample buffer. (B) Proteins were immunoprecipitated from the lysate with a polyclonal mouse serum recognizing RRV vp7, MB7 (B), or with the nonneutralizing MAb against VP7, M60 (60), and were separated by reducing SDS-PAGE. The positions of molecular mass markers (in kilodaltons) are indicated to the right of the gels. vp3/4, vp3 and vp4; ns34/35, ns34 and ns35.

vp7 from DTT-treated cells remained constant through the chase period, the mobility of vp7 from non-DTT-treated cells increased during the chase period (Fig. 4B). The difference in migration between DTT-treated and non-DTT-treated vp7 was confirmed by measuring their migration relative to that of vp6 on the negative. While DTT-treated vp7 migrated 6 mm further than vp6 did, non-DTT-treated vp7 migrated 8 mm further. This increase in the mobility of non-DTT-treated vp7 during a chase period has been observed previously and reflects the trimming of the oligosaccharide side chain of vp7 (31). As expected, no trimeric vp6 was observed in the boiled samples separated by reducing SDS-PAGE.

To examine the antigenicity of vp7 in these lysates, the vp7 protein was immunoprecipitated with the nonneutralizing MAb M60 or with the polyclonal antiserum MB7 and was analyzed by reducing SDS-PAGE. DTT treatment during rotavirus protein synthesis eliminated the M60 epitope on vp7 (Fig. 4C). M60 efficiently immunoprecipitates non-DTT-treated vp7 (Fig. 4C), indicating that the M60 epitope is dependent on a vp7 conformation requiring disulfide bonds. The loss of M60-precipitable vp7 does not reflect degradation of vp7, since the reduced protein was efficiently immunoprecipitated by the polyclonal antiserum MB7 (Fig. 4C). Apparently, MB7 recognized non-disulfide-dependent vp7 epitopes.

Glycosylation of rotavirus proteins in the presence of DTT. To determine if DTT treatment prevented N-linked glycosylation of rotavirus glycoprotein, tunicamycin (2 μg/ml) was added to methionine-free medium 1 h before metabolic pulse-labeling with [^{35}S]methionine in the presence of DTT and tunicamycin. vp7 and ns28 synthesized in the presence of 1 mM DTT but in the absence of tunicamycin migrated more slowly by reducing SDS-PAGE than did vp7 and ns28 synthesized in the presence of both DTT and tunicamycin (Fig. 5). These results indicate that disulfide bond formation in vp7 was not a prerequisite for its glycosylation and that dolichol phosphate transfer occurred in the presence of DTT. By comparison to Fig. 4B, there appears to have been some degradation of the vp7 in the lysates of both the tunicamycin-treated and non-tunicamycin-treated cells.

We had attributed the differences in reducing SDS-PAGE mobilities between DTT-treated and non-DTT-treated vp7 that emerged during a chase period (Fig. 4B) to differences in the trimming of the oligosaccharide side chain of vp7. Confirming this, metabolically labeled vp7, synthesized and chased for 120 min in the presence or absence of DTT, comigrated after endoglycosidase H treatment (data not shown).

Intracellular reoxidation restores the disulfide bonds and antigenicity of vp7. To determine if intracellular reoxidation could restore the folding and antigenicity of DTT-treated vp7,

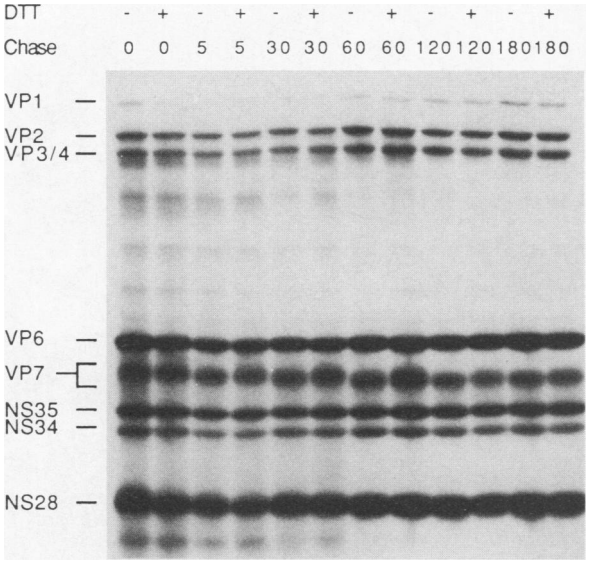

FIG. 7. Reducing SDS-PAGE of intracellularly reoxidized rotavirus proteins. At 7 h p.i., RRV-infected cells were methionine starved for 1 h and then treated with a 10-min [^{35}S]methionine pulse (50 μCi/ml) in the presence (+) or absence (−) of 1 mM DTT. Cells were either lysed immediately after the pulse or reoxidized in cell culture medium containing 10 mM added methionine and 0.7 mM cycloheximide for 5 to 180 min (as indicated over the lanes). Before lysis, monolayers were washed with ice-cold PBS–40 mM NEM. Samples were boiled for 3 min in reducing sample buffer before separation by SDS-PAGE. VP3/4, vp3 and vp4.

rotavirus-infected cells were metabolically pulse-labeled during DTT treatment, washed, and incubated in DTT-free chase medium for the indicated times (Fig. 6). Upon separation by nonreducing SDS-PAGE, reduced vp7 was identifiable in a lysate produced 5 min after a 10-min pulse-labeling in the presence of 1 mM DTT (Fig. 6A). However, after 30- and 60-min DTT-free chase periods, vp7 was no longer identifiable by nonreducing SDS-PAGE (Fig. 6A). The most likely explanation for the apparent loss of vp7 is that it had reoxidized and comigrated with ns34 and ns35 (as seen in Fig. 4A). When vp7 was pulse-labeled at the beginning of a 70-min DTT treatment, it remained identifiable by nonreducing SDS-PAGE throughout a 60-min DTT-free chase period (Fig. 6A). This result suggested that after 70 min of DTT treatment, vp7 was permanently misfolded and could no longer be fully oxidized to form a compact structure that comigrated with ns34 and ns35.

To test the above hypotheses and assay the antigenicity of reoxidized vp7, proteins were immunoprecipitated from the above lysates with M60 (a MAb that recognizes oxidized vp7) and MB7 (a polyclonal antiserum that recognizes vp7) and analyzed by reducing SDS-PAGE (Fig. 6B). The M60 epitope on vp7 treated with 1 mM DTT for 10 min was rapidly restored by a chase under nonreducing conditions (Fig. 6B). On the other hand, after 1 mM DTT treatment of vp7 for 70 min, little formation of the M60 epitope occurred during reoxidation.

To rule out the possibility that degradation of DTT-treated vp7 during the reoxidation period caused its disappearance on a gel under nonreducing conditions (Fig. 6A), vp7 was pulse-labeled for 10 min in the presence of 1 mM DTT, chased in the absence of DTT, and separated by reducing SDS-PAGE (Fig. 7). No significant degradation of vp7 was seen over a 180-min chase period (Fig. 7). At 0 and 180 min of oxidizing chase, vp7 synthesized in the presence or absence of DTT comigrated, although both proteins migrated further than vp6 and ns35 did after the chase period, reflecting trimming of the vp7 oligosaccharide side chain. However, at intermediate periods of oxidizing chase (5, 30, 60, and 120 min), the vp7 synthesized in the absence of DTT migrated more quickly than the vp7 synthesized in the presence of DTT (Fig. 7). These results suggest an approximately 60-min lag in the trimming of vp7 synthesized in the presence of DTT. DTT treatment of RRV-infected cells for 30 min before pulse-labeling in the absence of DTT did not affect the trimming of the pulse-labeled vp7, indicating that DTT treatment of vp7, not of the trimming enzymes, was responsible for the lag in the processing of DTT-treated vp7 (data not shown).

Intracellular DTT treatment blocks assembly of outer capsid proteins into mature 70-nm double-shelled particles. The effect of DTT treatment of rotavirus-infected MA104 cells on viral assembly was studied by electron microscopy. In samples fixed after treatment with 1 mM DTT from 6 to 9 h p.i., morphologically normal single-shelled particles were seen budding into the RER (Fig. 8A and B). A distinctive feature of the DTT-treated samples was the accumulation of 90- to 100-nm-enveloped particles in the RER (Fig. 8A, arrows) and the presence in the RER of 50-nm-particles with a ring-shaped appearance (Fig. 8B, arrows). This contrasts with the non-DTT-treated sample (Fig. 8C) in which most of the particles in the RER were of the 70-nm-double-shelled type, and relatively few enveloped particles were present. Given the accumulation of enveloped intermediate and single-shelled particles but not double-shelled particles in the RER of DTT-treated cells, it appears that DTT treatment of rotavirus-infected cells halted rotavirus maturation at the enveloped intermediate stage.

DISCUSSION

Treatment of purified rotavirus particles with 1 to 10 mM DTT did not inhibit HA or early steps in viral replication (cell binding and entry; Table 1). Given that treatment of SA11 rotavirus particles with sodium sulfite, a reagent that breaks disulfide bonds, eliminates HA (7), we hypothesized that DTT treatment failed to break rotavirus disulfide bonds. In fact, established disulfide bonds in rotavirus particles were resistant to reduction by 1 to 10 mM DTT at 37°C (Fig. 1, lanes 3 and 6). Relative resistance to reduction has been observed in other viral proteins, such as trimeric influenza virus HA, particularly when DTT treatment is performed in the extracellular environment (51).

In contrast to the insensitivity of assembled rotavirus particles to DTT treatment, DTT treatment of rotavirus-infected cells starting at 2 h p.i. blocked production of infectious rotavirus particles, but not rotavirus antigen (Fig. 2). This finding suggested that intracellular DTT treatment blocked rotavirus assembly. To explore the nature of this block, we examined the effect of in vivo DTT treatment on individual rotavirus proteins by immunohistochemical staining (Table 2 and Fig. 3). While epitopes on rotavirus proteins vp4, vp6, and ns28 formed in the presence of DTT, conformationally determined neutralization epitopes and an SDS-resistant nonneutralizing epitope on the ER-resident glycoprotein vp7 failed to form in the presence of DTT.

Similarly, by SDS-PAGE, the effect of intracellular DTT treatment was most pronounced on vp7. A brief DTT pulse did not prevent the synthesis of vp7 but did prevent the formation of its SDS-PAGE-detectable disulfide bonds (Fig. 4). Reduced influenza virus hemagglutinin can be reoxidized, allowing trimerization and reestablishment of correct epitopes (10).

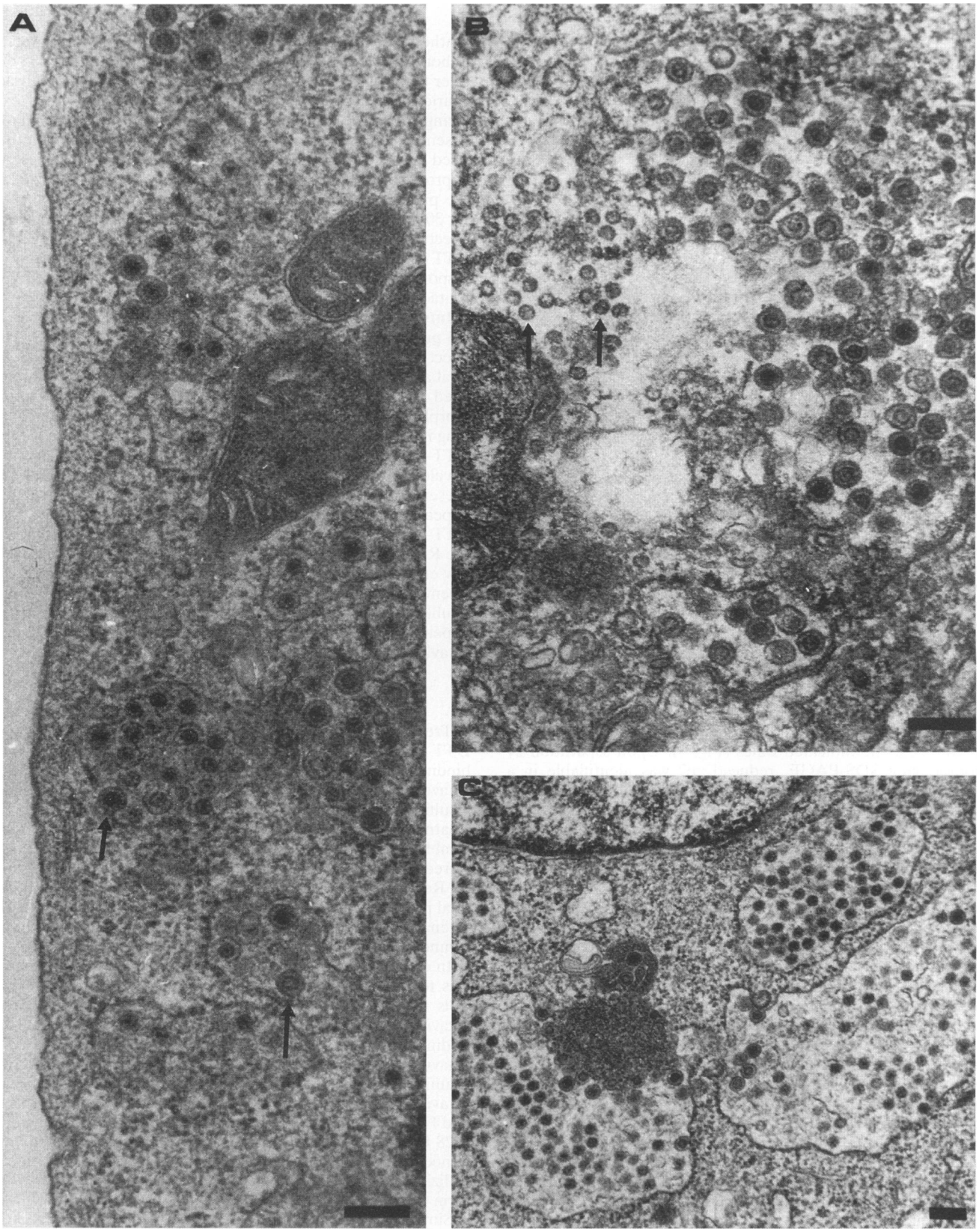

FIG. 8. Electron micrographs of DTT-treated or non-DTT-treated, RRV-infected MA104 cells. DTT-treated cells were incubated from 4 to 9 h p.i. in medium containing 1 mM DTT. The cells were fixed and processed for electron microscopy as described in Materials and Methods. Bars, 200 nm. (A) DTT-treated, RRV-infected MA104 cells. Note that single-shelled particles bud through the ER membrane to form enveloped intermediate particles (arrows). (B) DTT-treated, RRV-infected MA104 cells. Note the accumulation of 50-nm single-shelled-like particles in the lumen of the ER (arrows). (C) RRV-infected MA104 cells not treated with DTT.

Likewise, reoxidation of vp7 restored its antigenicity and proper mobility by nonreducing SDS-PAGE (Fig. 6). On the other hand, prolonged DTT treatment led to the accumulation of permanently misfolded vp7 (Fig. 6). The restoration of disulfide bonds following reduction demonstrates that disulfide bonds of vp7 can form posttranslationally.

DTT reduction did not inhibit N-linked glycosylation of either vp7 or ns28 (Fig. 5), consistent with results obtained in other systems (10, 13, 39). In the ER of rotavirus-infected cells, the high-mannose side chain of vp7 is trimmed (18, 31), resulting in a gradual increase in its electrophoretic mobility. Although vp7 expressed in DTT-treated cells was glycosylated, it failed to increase its mobility during a chase in the presence of DTT (Fig. 4B), indicating a lack of trimming. When vp7 synthesized in the presence of DTT was reoxidized, its trimming was delayed for approximately 60 min relative to that of non-DTT-treated vp7 (Fig. 7). These results suggest that trimming of vp7 oligosaccharide side chain occurs only after the formation of disulfide bonds.

Inhibition of the processing of the vp7 oligosaccharide side chain has also been observed in cells depleted of calcium with a calcium ionophore and in cells incubated with manganese, a calcium competitor (43). Since vp7 undergoes a calcium-dependent conformational change to acquire neutralizing epitopes (15), the final folding of vp7 was likely blocked by calcium ionophore or manganese treatment of infected cells. Furthermore, energy-dependent transport of vp7 to an ER subcompartment may be required for vp7 trimming (31). These data suggest that disulfide-bonded, calcium-bound, fully folded vp7 may be selectively processed by ER mannosidases, perhaps following transport to an ER subcompartment.

While in vivo DTT treatment had dramatic effects on vp7, its effects on other rotavirus proteins were more subtle. Immunoperoxidase staining for the 1A9 epitope on vp4 and the B4/55 epitope on ns28 were diminished but not eliminated in DTT-treated, RRV-infected MA104 cells (Table 2). While no dramatic shifts in the electrophoretic mobilities of these proteins by nonreducing SDS-PAGE were noted upon DTT treatment of infected cells, we cannot rule out the possibility of more subtle effects not apparent on the gels. For example, on polyacrylamide gels with a low percentage of polyacrylamide, we have observed in vitro reduction-induced shifts in the mobility of vp4 produced in RRV-infected cells treated with NEM before lysis (data not shown), consistent with intramolecular disulfide bonding. Two disulfide bonds have been mapped in vp4 from RRV-infected cells lysed with buffer containing iodoacetamide, a sulfhydryl blocking agent (40). The smaller effect of DTT treatment on vp4 than on vp7 may reflect a less essential role for disulfide bonds in the structure and function of vp4. Some infectious strains of rotavirus lack disulfide bonds either from the vp8 or vp5 trypsin cleavage fragments of vp4 (27, 40). In addition, it has been hypothesized that vp4 is added to nascent rotavirus particles in the cytoplasm (46), where the environment is too reducing to permit any but the most stable disulfide linkages to form (23). Therefore, disulfide bonds in vp4 may not be necessary for its assembly into particles.

Various researchers have found evidence for disulfide bonds in the rotavirus major inner capsid protein, vp6. Some evidence suggests intramolecular disulfide bonds (24, 40), while other evidence suggests intermolecular bonds (8, 19, 44). When we analyzed non-NEM-treated, purified particles by nonreducing SDS-PAGE, we saw evidence for multiple forms of vp6 differing in their intramolecular disulfide bonds (Fig. 1, lane 1); however, when free sulfhydryl groups were alkylated by treating the particles with NEM before disruption, only one form of vp6 was detected (Fig. 1, lane 2). In addition, we did not observe major differences in the nonreducing SDS-PAGE mobilities of vp6 obtained from DTT-treated and non-DTT-treated, RRV-infected MA104 cells (Fig. 4A and 6A). It is apparent that artifactual disulfide bonds readily form in vp6 during sample preparation, potentially accounting for the variability in the nature of vp6 disulfide bonds observed in previous studies, most of which have not employed agents that block free sulfhydryl groups. Nevertheless, on selected autoradiograms (data not shown), we have noted that boiling in β-mercaptoethanol slightly sharpens the band formed by NEM- or iodoacetamide-treated vp6, consistent with, though not conclusive for, the presence of intramolecular disulfide bonding in vp6. One previous study, which did employ a free sulfhydryl blocking agent (iodoacetamide), found evidence for intramolecular disulfide bonds in vp6 (40).

In any case, the vp6 trimer-specific MAb 255/60 (25, 33) bound vp6 synthesized in DTT-treated cells (Fig. 3), and nonboiled vp6 from DTT-treated cells migrated as a multimer, probably a trimer, by nonreducing SDS-PAGE (Fig. 4A). These results indicate that disulfide bonds are not required for trimer formation, consistent with the observation that established vp6 multimers are not disrupted by β-mercaptoethanol (24). If mature vp6, in fact, contains disulfide bonds, they likely form during the single-shelled particle's transit through the ER or extracellularly.

Electron microscopy further illuminated the role of disulfide bonds in rotavirus maturation (Fig. 8). In DTT-treated cells, single-shelled particles appeared to form properly and budded through the ER membrane, a process mediated by ns28, a virus-encoded ER transmembrane protein (5, 37). The translocated particles acquired an ER-derived membrane, but consistent with the block to vp7 antigenic maturation, no double-shelled particles were observed. Rather, membrane-enveloped intermediate particles accumulated. A similar block at the enveloped intermediate stage has been observed in tunicamycin-treated cells and in calcium ionophore-treated cells (41, 43). A recent electron micrographic study (48) has raised the possibility that enveloped particles are actually in a dead-end pathway and that outer capsid assembly occurs on single-shelled particles that directly penetrate the ER membrane. Future biochemical studies involving treatments, such as DTT treatment, that cause enveloped intermediate particles to accumulate may clarify the product-precursor relationships among the observed ER-associated subviral particles.

In summary, we observed that in vivo DTT treatment of RRV-infected cells inhibited vp7 antigenic maturation, trimming of oligosaccharides on vp7, and formation of the rotavirus outer capsid. All of these processes take place in the ER, consistent with the generalization that the ER is the site of disulfide bond formation for cellular proteins (6, 29). vp7 antigenic maturation involves a calcium-dependent folding from a form recognized only by nonneutralizing MAbs, such as M60, to a form like that on the outer capsid, presenting a full range of neutralizing epitopes (15, 16). Since the M60 epitope on vp7 is disulfide bond dependent, these experiments establish that disulfide bond formation precedes the calcium-dependent folding of vp7. Since the process of outer capsid formation remains incompletely understood, it is possible that effects of DTT on proteins other than vp7 contribute to the DTT-induced block of rotavirus maturation at the enveloped intermediate stage.

ACKNOWLEDGMENTS

We thank Steven Dunn and Tonja Cross for providing the polyclonal antiserum MB7 and Anssi Mörttinen for technical assistance.

This work was supported by Swedish Medical Research Council (K92-16P-10136-01A and B93-16X-10392-01A); by NIH grants R01 AI21362 and NRSA 5T32 AI07328; by the Stanford University Digestive Disease Center CDK38707, NIH, DDK; and by a VA Merit Review Grant.

REFERENCES

1. **Adams, W. R., and L. M. Kraft.** 1967. Electron-microscopic study of the intestinal epithelium of mice infected with the agent of epizootic diarrhea of infant mice (EDIM). Am. J. Pathol. **51:**39–60.
2. **Alberini, C. M., P. Bet, C. Milstein, and R. Sitia.** 1990. Secretion of immunoglobulin M assembly intermediates in the presence of reducing agents. Nature (London) **347:**485–487.
3. **Altenburg, B. C., D. Y. Graham, and M. K. Estes.** 1980. Ultrastructural study of rotavirus replication in cultured cells. J. Gen. Virol. **46:**75–85.
4. **Anfinsen, C. B., E. Haber, M. Sela, and F. White.** 1961. The kinetics of formation of ribonuclease during oxidation of the reduced polypeptide chain. Proc. Natl. Acad. Sci. USA **47:**1309–1314.
5. **Au, K. S., W. K. Chan, J. W. Burns, and M. K. Estes.** 1989. Receptor activity of rotavirus nonstructural glycoprotein NS28. J. Virol. **63:**4553–4562.
6. **Bardwell, J. C. A., and J. Beckwith.** 1993. The bonds that tie: catalyzed disulfide bond formation. Cell **74:**769–771.
7. **Bastardo, J. W., and I. H. Holmes.** 1980. Attachment of SA-11 rotavirus to erythrocyte receptors. Infect. Immun. **29:**1134–1140.
8. **Bastardo, J. W., J. L. Makimm-Breschin, S. Sonza, L. D. Mercer, and I. H. Holmes.** 1981. Preparation and characterization of antisera to electrophoretically purified SA-11 virus polypeptides. Infect. Immun. **34:**641–647.
9. **Braakman, I., H. Hoover-Litty, K. R. Wagner, and A. Helenius.** 1991. Folding of influenza hemagglutinin in the endoplasmic reticulum. J. Cell Biol. **114:**401–411.
10. **Braakman, U., J. Helenius, and A. Helenius.** 1992. Manipulating disulfide bond formation and protein folding in the endoplasmic reticulum. EMBO J. **11:**1717–1722.
11. **Collins, P. L., and G. Mottet.** 1991. Homo-oligomerization of the hemagglutinin-neuraminidase glycoprotein of human parainfluenza virus type 3 occurs before the acquisition of correct intramolecular disulfide bonds and mature immunoreactivity. J. Virol. **65:**2362–2371.
12. **Creighton, T. E.** 1978. Experimental studies of protein folding and unfolding. Prog. Drug. Res. **33:**231–297.
13. **De Silva, A., I. Braakman, and A. Helenius.** 1993. Posttranslational folding of vesicular stomatitis virus G protein in the ER: involvement of noncovalent and covalent complexes. J. Cell Biol. **120:**647–655.
14. **Doig, A. J., and D. H. Williams.** 1991. Is the hydrophobic effect stabilizing or destabilizing in proteins? The contribution of disulphide bonds to protein stability. J. Mol. Biol. **217:**389–398.
15. **Dormitzer, P. R., and H. B. Greenberg.** 1992. Calcium chelation induces a conformational change in recombinant herpes simplex virus-1-expressed rotavirus vp7. Virology **189:**828–832.
16. **Dormitzer, P. R., D. Y. Ho, E. R. Mackow, E. S. Mocarski, and H. B. Greenberg.** 1992. Neutralizing epitopes on herpes simplex virus-1-expressed rotavirus VP7 are dependent on coexpression of other rotavirus proteins. Virology **187:**18–32.
17. **Dorner, A. J., D. G. Bole, and R. J. Kaufman.** 1987. The relationship of N-linked glycosylation and heavy chain-binding protein association with the secretion of glycoproteins. J. Cell Biol. **105:**2665–2674.
18. **Ericson, B. L., D. Y. Graham, B. B. Mason, H. H. Hanssen, and M. K. Estes.** 1983. Two types of glycoprotein precursors are produced by the simian rotavirus SA11. Virology **127:**320–332.
19. **Estes, M. K., S. E. Crawford, M. E. Penaranda, B. L. Petrie, J. W. Burns, W. K. Chan, B. Ericson, G. E. Smith, and M. D. Summers.** 1987. Synthesis and immunogenicity of the rotavirus major capsid antigen using a baculovirus expression system. J. Virol. **61:**1488–1494.
20. **Freedman, R.** 1987. Protein chemistry. Folding into the right shape. Nature (London) **329:**196–197.
21. **Freedman, R. B., N. J. Bulleid, H. C. Hawkins, and P. L. Paver.** 1989. Role of protein disulfide-isomerase in the expression of native proteins. Biochem. Soc. Symp. **55:**167–192.
22. **Gething, M. J., and J. Sambrook.** 1992. Protein folding in the cell. Nature (London) **355:**33–45.
23. **Gilbert, H. F.** 1990. Molecular and cellular aspects of thiol-disulfide exchange. Adv. Enzymol. **63:**69–172.
24. **Gorziglia, M., C. Larrea, F. Liprandi, and J. Esparza.** 1985. Biochemical evidence for the oligomeric (possible trimeric) structure of the major inner capsid polypeptide (45k) of rotaviruses. J. Gen. Virol. **66:**1889–1900.
25. **Greenberg, H. B., V. McAuliffe, J. Valdesuso, R. Wyatt, J. Flores, A. Kalica, Y. Hoshino, and N. Singh.** 1983. Serological analysis of the subgroup protein of rotavirus, using monoclonal antibodies. Infect. Immun. **39:**91–99.
26. **Greenberg, H. B., J. Valdesuso, K. van Wyke, K. Midthun, M. Walsh, V. McAuliffe, R. G. Wyatt, A. R. Kalica, J. Flores, and Y. Hoshino.** 1983. Production and preliminary characterization of monoclonal antibodies directed at two surface proteins of rhesus rotavirus. J. Virol. **47:**267–275.
27. **Hardy, M. E., M. Gorziglia, and G. N. Woode.** 1992. Amino acid sequence analysis of bovine rotavirus B223 reveals a unique outer capsid protein VP4 and confirms a third bovine VP4 type. Virology **191:**291–300.
28. **Harlow, E., and D. Lane.** 1988. Antibodies. A laboratory manual. Cold Spring Harbor Laboratory, Cold Spring Harbor, N.Y.
29. **Hwang, C., A. J. Sinskey, and H. F. Lodish.** 1992. Oxidized redox state of glutathione in the endoplasmic reticulum. Science **257:**1496–1502.
30. **Jaenicke, R.** 1991. Protein folding: local structures, domains, subunits, and assemblies. Biochemistry **30:**3147–3161.
31. **Kabcenell, A. K., and P. A. Atkinson.** 1985. Processing of the rough endoplasmic reticulum membrane glycoproteins of rotavirus SA-11. J. Cell Biol. **101:**1270–1280.
32. **Kalica, A. R., H. D. James, and A. Z. Kapikian.** 1978. Hemagglutination by simian rotavirus. J. Clin. Microbiol. **7:**314–315.
33. **Liprandi, F., G. Lopez, I. Rodriguez, M. Hidalgo, J. E. Ludert, and N. Mattion.** 1990. Monoclonal antibodies to the VP6 of porcine subgroup I rotaviruses reactive with subgroup I and non-subgroup I, non-subgroup II strains. J. Gen. Virol. **71:**1395–1398.
34. **Lodish, H. F., N. Kong, and L. Wikstrom.** 1992. Calcium is required for folding of newly made subunits of the asialoglycoprotein receptor within the endoplasmic reticulum. J. Biol. Chem. **267:**12753–12760.
35. **Maass, D. R., and P. H. Atkinson.** 1990. Rotavirus proteins VP7, NS28, and VP4 form oligomeric structures. J. Virol. **64:**2632–2641.
36. **Mackow, E. R., R. D. Shaw, S. M. Matsui, P. T. Vo, M. N. Dang, and H. B. Greenberg.** 1988. The rhesus rotavirus gene encoding protein VP3: location of amino acids involved in homologous and heterologous rotavirus neutralization and identification of a putative fusion region. Proc. Natl. Acad. Sci. USA **85:**645–649.
37. **Meyer, J. C., C. C. Bergmann, and A. R. Bellamy.** 1989. Interaction of rotavirus cores with the nonstructural glycoprotein NS28. Virology **171:**98–107.
38. **Michelangeli, F., M.-C. Ruiz, J. Castillo, J. Ludert, and F. Liprandi.** 1991. Effect of rotavirus on intracellular calcium homeostasis in cultured cells. Virology **181:**520–527.
39. **Opstelten, D.-J. E., P. de Groote, M. C. Horzinek, H. Vennema, and P. J. M. Rottier.** 1993. Disulfide bonds in folding and transport of mouse hepatitis coronavirus glycoproteins. J. Virol. **67:**7394–7401.
40. **Patton, J. T., J. Hua, and E. A. Mansell.** 1993. Location of intrachain disulfide bonds in the VP5* and VP8* trypsin cleavage fragments of the rhesus rotavirus spike protein VP4. J. Virol. **67:**4848–4855.
41. **Petrie, B. L., M. K. Estes, and D. Y. Graham.** 1983. Effects of tunicamycin on rotavirus morphogenesis and infectivity. J. Virol. **46:**270–274.
42. **Petrie, B. L., H. B. Greenberg, D. Y. Graham, and M. K. Estes.** 1984. Ultrastructural localization of rotavirus antigens using colloidal gold. Virus Res. **1:**133–152.
43. **Poruchynsky, M. S., D. R. Maass, and P. H. Atkinson.** 1991. Calcium depletion blocks the maturation of rotavirus by altering

the oligomerization of virus-encoded proteins in the ER. J. Cell Biol. **114**:651–661.
44. **Sabara, M., K. F. M. Ready, P. J. Frenchick, and L. A. Babiuk.** 1987. Biochemical evidence for the oligomeric arrangement of bovine rotavirus nucleocapsid protein and its possible significance in the immunogenicity of this protein. J. Gen. Virol. **68**:123–133.
45. **Shahrabadi, M. S., L. A. Babiuk, and P. W. K. Lee.** 1987. Further analysis of the role of calcium in rotavirus morphogenesis. Virology **158**:103–111.
46. **Shaw, A. L., R. Rothnagel, D. Chen, R. F. Ramig, W. Chiu, and B. V. V. Prasad.** 1993. Three-dimensional visualization of the rotavirus hemagglutinin structure. Cell **74**:693–701.
47. **Shaw, R. D., P. T. Vo, P. A. Offit, B. S. Coulson, and H. B. Greenberg.** 1986. Antigenic mapping of the surface proteins of rhesus rotavirus. Virology **155**:434–451.
48. **Suzuki, M., T. Konno, and Y. Numazaki.** 1993. Electron microscopic evidence for budding process-independent assembly of double-shelled rotavirus particles during passage through endoplasmic reticulum membranes. J. Gen. Virol. **74**:2015–2018.
49. **Svensson, L., H. Sheshberadaran, S. Vene, E. Norrby, M. Grandien, and G. Wadell.** 1987. Serum antibody responses to individual viral polypeptides in human rotaviruses infections. J. Gen. Virol. **68**:643–651.
50. **Taniyama, Y., R. Kuroki, F. Omura, C. Seko, and M. Kikuchi.** 1991. Evidence for intramolecular disulfide bond shifting in the folding of mutant human lysozyme. J. Biol. Chem. **266**:6456–6461.
51. **Tatu, U., I. Braakman, and A. Helenius.** 1993. Membrane glycoprotein folding, oligomerization and intracellular transport: effects of dithiothreitol in living cells. EMBO J. **12**:2151–2157.
52. **Tian, P., Y. Hu, W. P. Schilling, D. A. Lindsay, J. Eiden, and M. K. Estes.** 1994. The nonstructural glycoprotein of rotavirus affects intracellular calcium levels. J. Virol. **68**:251–257.